Comparison of Electric Field of Corona Discharge in Single-Wire- and Multi-Wire-to-Plate Electrode Systems

P. Marciulionis, S. Zebrauskas

Department of Electrical Engineering, Kaunas University of Technology,
Studentų st. 48, LT-51367 Kaunas, Lithuania, phone:+370 37 300268; e-mail: povilas.marciulionis@ktu.lt

Introduction

Direct current corona discharge is often used in many industry applications. Corona discharge electrode represented by thin wire or a needle charges small particles and liquid droplets. Some of corona discharge devices have electrode systems with many corona electrodes to have more charged particles or to control trajectories of their motion. Many geometrical forms of corona discharge electrode could be wires, pins, needles and another. The corona discharge electric field of multi-corona electrode system is different from single corona electrode system. The charge of each electrode produces electric field and influences another electrode field. To compute this field this influence must be assessed.

Other researchers tried to solve this problem long before [1]. Nowadays there are many experimental research results of the discharge in multi-electrode systems. They involve bacterium cleaning in drinking water [2], the effect of the air flow in multi-electrode corona field [3], enhancement of drying effect [4], ozone generation characteristics in multi-point corona electrodes [5], etc.

Some authors have tried various ways to solve this problem theoretically. Several of them invoke a commercial software packages with finite element method FEMLAB, COMSOL or ANSYS [6, 7], the other calculate with their made programs using numerical [8, 9] or analytical [10] methods.

It is clear from their results that in each corona discharge electrode system electric field are quite different. It must be simulated separately to each application of the corona field.

In this paper we show differences and similarities of the corona field in single-wire and multi-wire-to-plate electrodes system. Information of the electric field distribution in these systems in some cases may determine the creation of more precision and economical systems.

We present there the results of field simulation numerical model based on the finite difference method in the software environment of the package DELPHI.

Numerical modeling of corona discharge electric field

We selected the polar coordinate system for numerical simulation of the corona field due to the reasons which were mentioned in our previous papers [11]. Single-wire-to-plate electrode system is shown in Fig. 1. Computational grid of multi-wire-to-plate corona discharge electrode system is shown in Fig. 2. Distances of the computational grid are regular near the corona electrode. At the right side of the computation field the distances are irregular for both electrode systems. Irregular distances of the computational grid are also near the plate electrode.

Analysis of the corona field consists of two equations: the Poisson equation (1) and charge conservation equation (2):

$$\mathrm{divgrad}V = -\frac{\rho}{\varepsilon}, \qquad (1)$$

$$\mathrm{grad}\rho \cdot \mathrm{grad}V = \frac{\rho^2}{\varepsilon}. \qquad (2)$$

Finite-difference approximation of the Poisson equation for polar grid contains potential differences related to distances a_P, … a_S between central grid node O and neighbor nodes P, R, Q, S (see Fig. 1) and depends on the spatial charge located at the central node O

$$\frac{2V_P}{a_P^2 + a_P a_R} + \frac{2V_R}{a_R^2 + a_P a_R} + \frac{2V_Q}{a_Q^2 + a_Q a_S} + \frac{2V_S}{a_S^2 + a_Q a_S} + \frac{a_S V_Q}{r_1(a_Q^2 + a_Q a_S)} -$$

$$- \frac{a_Q V_S}{r_1(a_S^2 + a_Q a_S)} - V_O\left(\frac{2}{a_Q a_S} + \frac{2}{a_R a_P} + \frac{a_S^2 - a_Q^2}{r_1(a_Q a_S^2 + a_S a_Q^2)}\right) = -\frac{\rho_O}{\varepsilon}. \quad (3)$$

Differential equation of charge conservation is of the following form

$$\frac{\partial \rho}{\partial r}\cdot\frac{\partial V}{\partial r}+\frac{1}{r}\frac{\partial \rho}{\partial \varphi}\cdot\frac{1}{r}\frac{\partial V}{\partial \varphi}=\frac{\rho^2}{\varepsilon}. \qquad (4)$$

Difference form of this equation is given in [11].

It is clear from (4) that spatial charge located at the central node O depends on special charge and potential partial derivatives product.
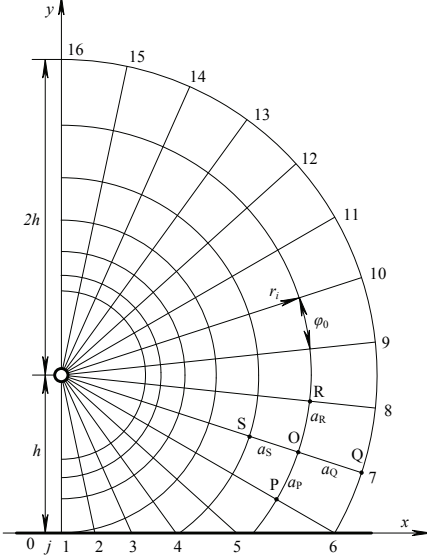

Fig. 1. Polar grid in single-wire-to-plane electrode system

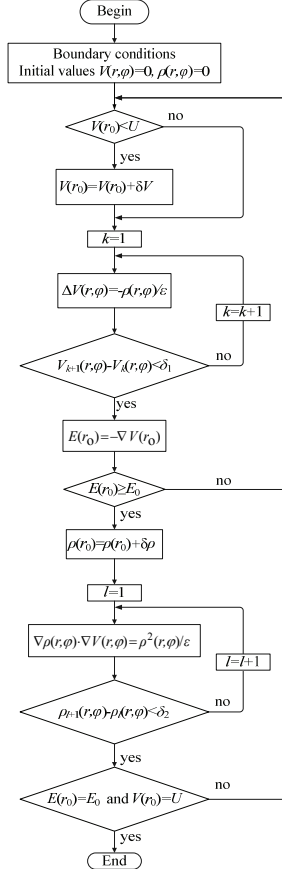An algorithm of corona field numerical analysis is shown in Fig. 2.

Fig. 2. Algorithm of corona field numerical analysis

Boundary conditions in multi-wire electrode system

Boundary conditions in single-wire electrode system were shown in our paper [11]. All boundary conditions in multi-wire-to-plane electrode system are the same, except boundary condition at the right side (line $x = g$, Fig. 3).
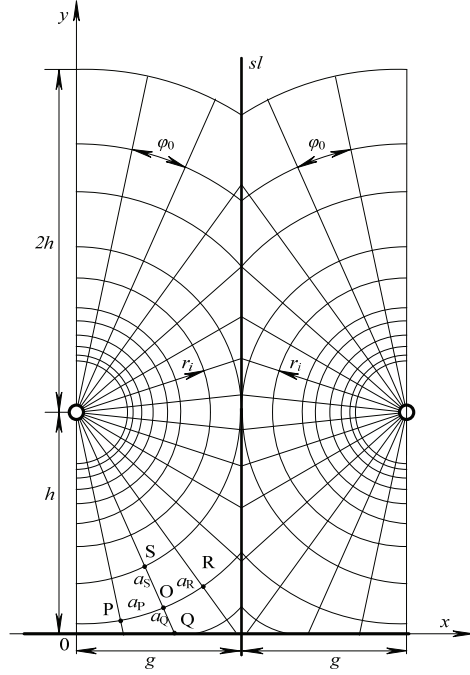

Fig. 3. Polar grid in multi-wire-to-plane electrode system

We assume in this paper that all corona discharge electrodes are of the same potential, distances to the plane are the same also. Polar grid element at the boundary is shown in Fig. 4. Because of condition mentioned above it is clear that line sl shown in Fig. 3 is the symmetry line and the potentials and space charges are equal $V_S = V_Q$, $\rho_S = \rho_Q$. We insert new point G to the computational grid between four computational grid points. This point G is located on the perpendicular line to the symmetry line sl between points S and S′. So new rectangular five point grid with irregular distances between R, S, S′, P and the central G (Fig. 4) is obtained

$$\frac{2V_P}{a_P^2+a_Pa_R}+\frac{2V_R}{a_R^2+a_Pa_R}+\frac{2V_Q}{a_Q^2+a_Qa_S}+\frac{2V_S}{a_S^2+a_Qa_S}-$$
$$-V_G\left(\frac{2}{a_Qa_S}+\frac{2}{a_Ra_P}\right)=-\frac{\rho_G}{\varepsilon}. \qquad (5)$$

To compute potential value on the computational grid point O we assume that variation of electric potential between the points G and R along the symmetry line sl is uniform. Therefore the potential on the point O may be expressed as follows

$$V_O = V_G + \frac{V_R - V_G}{a_{RG}}\cdot a_{OG}, \qquad (6)$$

where a_{RG} is the distance between points R and G, and a_{OG} represents the distance between points O and G.
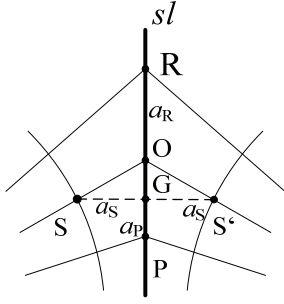
Fig. 4. Polar grid element at the boundary with irregular distances

The same principle is applied to irregular distances a_R and a_P on the symmetry line *sl*. Computational points situation is shown in Fig. 5.
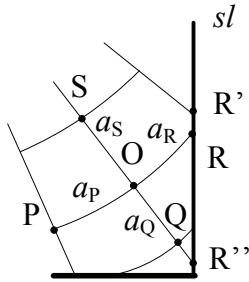

Fig. 5. Polar grid element at the boundary when the distance a_R is irregular

Potential of the point R

$$V_R = V_{R'} - \frac{V_{R'} - V_{R''}}{a_{R'R''}} \cdot a_{R'R} , \qquad (7)$$

where $a_{R'R''}$ is the distance between points R′ and R″; $a_{R'R}$ is the distance between points R′ and R; V_R, $V_{R'}$, $V_{R''}$ are the potentials of these points.

Boundary conditions for Poisson's equation (3) and the equation (4) are of Dirichlet type $V(r_0) = U$ and $V(y=0) = 0$. Boundary conditions on the surface of the wire are formed according the Kaptzov's assumption, which states that the corona field strength on the surface of wire electrode is constant and equal to its value E_0 corresponding to the inception voltage U_0 of the discharge $E(r_0) = E_0$.

Parameters of wire-to-plane electrode system are: radius of the wire $r_0 = 0{,}05$ mm, spacing between the wire and the plane electrode $h = 12{,}0$ mm The distance between the center of the wire and the symmetry line *sl* in the multi-wire-to-plane electrode system $g = 7{,}5$ mm.

Comparison of the electric field

Comparison of corona field in electrode systems shown in Fig. 1 and Fig. 2 is performed for points of the wire surface and for points of the first line of the computational area (line $x = 0$).

Corona field strength on the surface of the wire is constant and equal to $E(r_0) = E_0$ in both cases. Space charge density depends on given voltage of the wire and on the geometry of the electrodes. It is clear from Fig. 6

that space charge density near the surface of the wire in multi-wire electrode system is less in comparison with the value of wire-to-plane system and this difference increases with the angle. It is caused by the influence of the electric field of neighbor electrode. Space charge reduces electric field strength and sustains the value field strength to meet Kaptzov's assumption. Because of the condition that neighbor wire voltage is of the same value and of the same sign electric field between them reduces and the space charge density on the corona discharge electrode reduces significantly.
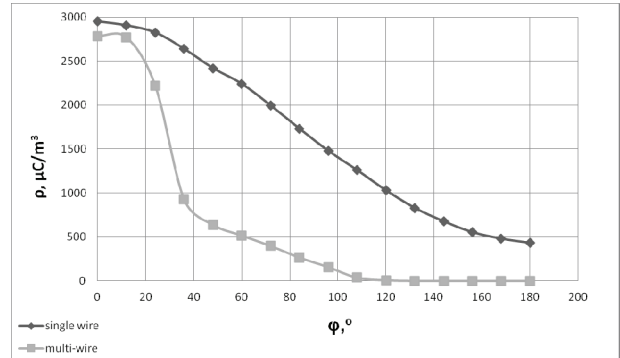

Fig. 6. Space charge density on the surface of the wire in single- and multi-wire-to-plane electrode systems

Space charge density on the surface of the wire decreases from points on the symmetry axis $x = 0$ to the other points on this surface. It is clear from the Fig. 6.
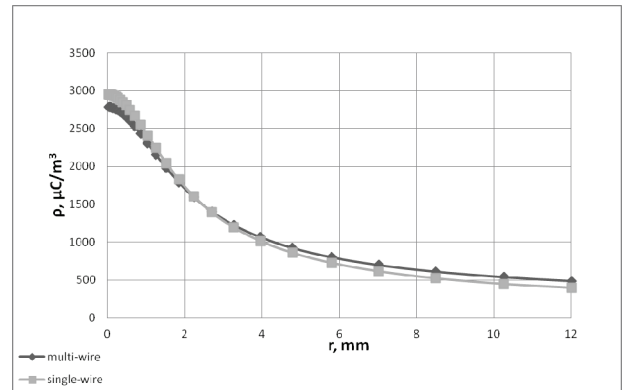

Fig. 7. Space charge density on the first line $j = 1$ of the computational area in single-wire- (Fig. 1) and multi-wire-to-plane (Fig. 2) electrode systems

Distribution of space charge density (Fig. 7) on the first line of computational area is of the same character for both compared systems.

Space charge density near the wire electrode it is less in the multi-wire-electrode system and it is a little greater near the plane.

The character of corona field strength distribution on the first line of the computational area (Fig. 8) is similar in both systems. Electric field strength on the surface of the wire is estimated from Peek′s law. It depends upon the geometry of the wire and an ambient air parameters. At the middle of the distance between wire and the plate electric field strenght is slightly weaker and near the plate is stronger in the multi-wire-to-plate electrode system.
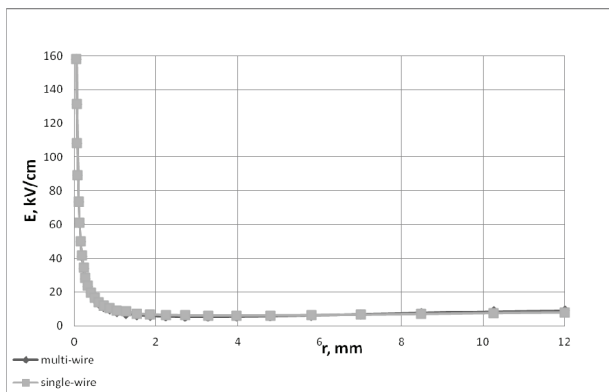
15

Fig. 8. Electric field strength on the first line of the computational area in single-wire- and multi-wire-to-plane electrode systems

Conclusions

The boundary condition differences are given for single and multi-wire-to-plane electrode systems.

Results of numerical corona field modeling in single- and multi-wire-to-plane electrode systems were compared for points on the surface of wire. Space charge density differs because of acting of neighbor wire fields. Space charge density on the surface of the wire in the multi-wire-to-plane electrode system is smaller.

Distribution of the space charge density on the first line of the computational area has no significant difference in both systems.

Corona field strength on the surface of the wire is constant according to Kaptzov's assumption. The character of corona field distribution on the symmetry line of the field has no significant difference.

References

1. **Elmoursi A. A., Castle P. G. S**. Modeling of corona characteristics in a wire–duct precipitator using the charge simulation technique // IEEE transaction on industry application, 1987. – Vol. IA–23. – No. 1. – P. 95–102.
2. **Cui–hua Wang, Yan Wu, Xin–qiang Shen.** A multi–wire–to–cylindrical type packed–bed plasma reactor for the inaction of M. aeruginosa // Journal of Electrostatics, 2010. – Vol. 68. – Iss. 1. – P. 31–35.
3. **Chun–Sheng Ren, Teng–Cai Ma, De–Zhen Wang, Jia–Liang Zhang, You–Nian Wang.** A study of cross–gas–flow to stabilize an atmospheric pressure glow plasma in a multi–pin–to–multi–cupped–plane // Journal of Electrostatics, 2006. – Vol. 64. – Iss. 1. – P. 23–28.
4. **Lai F. C., Sharma R. K.,** EHD–enhancement drying with multiple needle electrode // Journal of Electrostatics, 2005. – Vol. 63. – Iss. 3–4. – P. 23–28.
5. **Suarasan I., Ghizdavu L., Ghizdavu I., Sorin Budu, Dascalescu L.** Experimental characterization of multi–point corona discharge devices for direct ozonization of liquids // Journal of Electrostatics, 2002. – Vol. 54. – Iss. 2. – P. 207–214.
6. **Rickard M., Dunn–Rankin D.** Numerical simulation of a tubular ion–driven wind generator // Journal of Electrostatics, 2007. – Vol. 65. – Iss. 10–11. – P. 646–654.
7. **Kasayapanand N.,** Numerical modeling of the effect of number of electrodes on natural convection in an EHD fluid // Journal of Electrostatics, 2007. – Vol. 65. – Iss. 7. – P. 465–474.
8. **Barčiauskas R., Žebrauskas S.** Boundary conditions for combined corona and electrostatic field analysis in multi–electrode systems // Proceedings of the 5 th international conference on Electrical and Control Technologies. – Kaunas: Technologija, 2011. – P. 264–267.
9. **Zhang J., Lai F. C.** Effect of emitting electrode number on the performance of EHD gas pump in rectangular channel // Journal of Electrostatics, 2011. – Vol. 69. – Iss. 6. – P. 486–493.
10. **Ieta C. A., Kucerovsky Z., Greason W. D.** Current density modeling of a linear pin–plate array corona discharge // Journal of Electrostatics, 2008. – Vol. 66. – Iss. 11–12. – P. 589–593.
11. **Gudzinskas J.**, **Marciulionis P., Zebrauskas S.** Computation of electric wind parameters in direct current corona field // Electronics and Electrical Engineering. – Kaunas: Technologija, 2011. – No. 4(110). – P. 3–6. DOI: 10.5755/j01.eee.110.4.275.

P. Marciulionis, S. Zebrauskas. Comparison of Electric Field of Corona Discharge in Single-Wire- and Multi-Wire-to-Plate Electrode Systems // Electronics and Electrical Engineering. – Kaunas: Technologija, 2012. – No. 5(121). – P. 13–16.

Digital model for analysis of two-dimensional direct current corona field of single-wire-to-plane and multi-wire-to-plane electrode system is discussed. Finite-difference method in polar coordinate system is used for corona field computation. Differences of these fields boundary conditions are presented. Space charge density distribution at the surface of the wire and at the symmetry line is compared. Space charge density differs because of acting of neighbor wire fields. Comparison of field distribution is performed for the symmetry line because of the field strength is approximately constant on the wire surface according the Kaptzov's assumption. Ill. 8, bibl. 11 (in English; abstracts in English and Lithuanian).

P. Marčiulionis, S. Žebrauskas. Vainikinio išlydžio elektrinio lauko palyginimas elektrodų sistemose *laidas šalia plokštumos* ir *daugialaidė sistema šalia plokštumos* // Elektronika ir elektrotechnika. – Kaunas: Technologija, 2012. – Nr. 5(121). – P. 13–16.

Analizuojami ir lyginami elektrodų sistemos *laidas šalia plokštumos* ir *daugialaidė elektrodų sistema šalia plokštumos* dvimačio vienpolio vainikinio išlydžio elektrinio lauko skaitiniai modeliai. Elektrinis laukas abiem atvejais skaičiuojamas polinėje koordinačių sistemoje baigtinių skirtumų metodu. Pateikti šių sistemų kraštinių sąlygų skirtumai. Palygintas erdvinio krūvio tankio pasiskirstymas elektrodo paviršiuje ir simetrijos ašyje. Daugiaelektrodėje sistemoje gretimo elektrodo elektrinis laukas turi įtakos erdvinio krūvio pasiskirstymui. Pateiktas tik elektrinio lauko stiprio pasiskirstymas simetrijos ašyje, nes pagal Kaptzovo prielaidą elektrodo paviršiuje jis yra pastovus. Il. 8, bibl. 11 (anglų kalba; santraukos anglų ir lietuvių k.).